Symmetry and Electronic Structure of Noble-Metal Nanoparticles and the Role of Relativity

Hannu Häkkinen

Department of Physics, NanoScience Center, FIN-40014 University of Jyväskylä, Finland

Michael Moseler

Fraunhofer Institute for Mechanics of Materials, Wohlerstraße 11, D-79108 Freiburg, Germany

Oleg Kostko, Nina Morgner, Margarita Astruc Hoffmann, and Bernd v. Issendorff

Fakultät für Physik, Universität Freiburg, Stefan-Meier-Straße 21, D-79104 Freiburg, Germany
(Received 7 April 2004; published 27 August 2004)

We present high resolution UV-photoelectron spectra of cold mass selected Cu_n^-, Ag_n^-, and Au_n^- with $n = 53$–58. The observed electron density of states is not the expected simple electron shell structure, but is strongly influenced by electron-lattice interactions. Only Cu_{55}^- and Ag_{55}^- exhibit highly degenerate states. This is a direct consequence of their icosahedral symmetry, as is confirmed by density functional theory calculations. Neighboring sizes exhibit perturbed electronic structures, as they are formed by removal or addition of atoms to the icosahedron and therefore have lower symmetries. Gold clusters in the same size range show completely different spectra with almost no degeneracy, which indicates that they have structures of much lower symmetry. This behavior is related to strong relativistic bonding effects in gold, as demonstrated by *ab initio* calculations for Au_{55}^-.

Understanding the energetically most favorable structures that aggregates of metal atoms inherently adopt during their formation process is one of the long-standing issues in the science of clusters and nanoparticles [1,2]. The atomic structure and its symmetry are intimately related to the electronic structure, which in turn defines the electrical, optical and chemical properties of the particle. Resolving the atomic structures of nanoclusters therefore represents an important preliminary for their controlled use in future nanotechnologies. Noble-metal clusters and nanoparticles have attracted much attention recently as they are considered promising candidates for applications, e.g., in catalysis [3,4], labeling [5], or photonics [6]. Two size ranges of these particles have been characterized in detail: small clusters with up to 21 atoms have been studied by high resolution photoelectron and optical spectroscopy as well as a number of theoretical studies [7–14]. The results show that in this still rather "molecular" size range the clusters tend to adopt a variety of low-symmetry structures (the tetrahedral Au_{20}^- being a prominent exception [14]). Much larger particles, with hundreds or thousands of atoms, have been studied by electron microscopy and electron diffraction [15,16]. It turned out that these particles adopt well-ordered structures with surprisingly diverse overall symmetries. Icosahedral, decahedral, and (bulklike) octahedral forms are often observed at the same time, with the preferred structural motif depending sensitively on the particle formation process. Experimental structural information for medium sized (around 50 atoms and up) Cu, Ag, and Au clusters was scarce up to now. Measurements of ionization potentials [17] and UV-photoelectron spectroscopy studies [18] gave evidence

for the existence of some free-electron shell structure, which lead to the general perception that the properties of noble-metal clusters in this size range can be fully explained by the free-electron model.

We have performed high resolution photoelectron spectroscopy on free, cold, size selected noble-metal clusters at a photon energy of 6.42 eV. The setup is the same as used in earlier experiments [19,20]. Its electron spectrometer has an energy resolution of about $E/dE = 40$. It has been calibrated by measuring the known spectra of the monomer anions, which leads to an error of the energy axis of less than 30 meV. Typically, the photoelectron spectra have been averaged over 30 000 laser shots. We estimate the temperature of the clusters to be 200 ± 50 K.

The spectra obtained for Cu_n^-, Ag_n^-, and Au_n^- with $n = 53$–58 are shown in Fig. 1. In principle these are direct images of the electronic density of states. In the bulk the electronic structure of noble metals is characterized by a half-filled and rather free-electron like band formed from the atomic s orbitals, overlapped some eV below the Fermi energy by the so-called d band, which is formed from the rather localized atomic d orbitals. As has been discussed in detail already by Taylor *et al.* [18], this structure is clearly visible in the photoelectron spectra: the uppermost part of the distributions can be identified as being dominantly s electron derived, while the onset of the d bands can be observed roughly 2–3 eV below the uppermost state. The s-band part of the electronic density of states should therefore exhibit the same discrete structure as observed, e.g., for alkali clusters [1,20]. The 57-atom cluster anions contain 58 valence s electrons, and in the spherical droplet approximation should have the

closed shell configuration $1S^2 1P^6 1D^{10} 2S^2 1F^{14} 2P^6 1G^{18}$ (for clarity we refer to free-electron angular momentum states with a capital letter). Adding one atom should lead to the appearance of a singly occupied 2D orbital. Indeed for all three metals a new peak appears for size 58, which indicates the formation of a new shell. However, the free-electron model also predicts that in the section of the *s* band visible here only four shells should be present: $1F$, $2P$, $1G$, and $2D$. The structure of the photoelectron spectra obviously is more complicated than that, which hints at a relatively strong perturbation of the shell structure by electron-lattice interaction. The only clusters exhibiting a clear structure of highly degenerate states are Cu_{55}^- and Ag_{55}^-. Such degeneracies can be produced only by a highly symmetric atomic structure. Au_{55}^-, on the other hand, exhibits a complex spectrum without significant level bunching; it therefore seems not to adopt any of the atomic symmetries that lead to pronounced degeneracy of electron shells. This is in accordance with earlier mass spectroscopic measurements which demonstrated that 55 is a strong atomic magic number for silver, but not for gold [21,22]. Nevertheless the photoelectron spectrum of Au_{55}^- (like those of the other clusters) is absolutely reproducible and does not depend on source conditions, which indicates that all the clusters studied had just one or at least only a small number of definite structures.

The atomic and electronic structures of silver and gold clusters were calculated by density functional theory in combination with Born-Oppenheimer molecular dynam-

ics [23], including self-consistent gradient corrections [24]. The interaction of the $d^{10} s^1$ valence electrons of Ag and Au with the atomic cores was described by scalar-relativistic norm-conserving pseudopotentials [25]. For Au a nonrelativistic pseudopotential was used as well, in order to check the influence of relativity. The Kohn-Sham orbitals were expanded in a plane wave basis with a kinetic energy cutoff of 62 Ry. The method does not employ a supercell, and is thus suitable for accurate calculations for charged finite clusters [23]. As a full simulated-annealing scheme with *ab initio* determination of the electronic structure at each dynamic step still is computationally too expensive for this size of *d*-metal clusters (having a total number of valence electrons of about 600), we adopted an alternative strategy. We made use of the already existing knowledge about possible structures of nanosized metal clusters, which has been obtained by simulated annealing and genetic algorithm optimization of clusters described by classical pairwise and many-atom interatomic potentials. An extensive collection of such structures, known as the Cambridge Cluster Database (CCD), is publicly available on the World Wide Web [26]. For the structural optimization of Ag_{55}^- and Au_{55}^- we chose six candidates representing different structural motifs: closed atomic shell icosahedral (ICO), decahedral (DECA), and cuboctahedral (CUBO) structures, and the optimum structures found for classical Sutton-Chen (SC), glue (GL), and Morse (MO) potentials. These geometries were then optimized by *ab initio* molecular dynamics simulations, allowing the clusters to relax for 1 ps under the influence of a global friction force. In none of the cases this relaxation lead to a severe change of the overall structure.

The optimized structures and their electronic densities of states (DOS) as well as the measured spectra are shown in Fig. 2. One can see that in the case of Ag_{55}^- only two of them, the icosahedron [27] and the cuboctahedron, show a clear shell structure such as the one observed in the experiment. All other isomers exhibit much less distinct level bunching. Of the six structures considered, the icosahedral cluster ICO is the clear ground state. Its calculated DOS matches very well the experimental photoelectron spectrum. This allows us to identify the shells visible in the measured spectrum as the icosahedral orbitals $T_{2u}^6 G_u^8 T_{1u}^6 H_g^{10} G_g^6$. These levels can be seen as being produced from the angular momentum eigenstates of the spherical droplet by crystal field splitting [28,29]. The lattice of the cluster represents a perturbing potential of icosahedral symmetry. Group theory tells us that such a perturbation does not lift the degeneracy of the 2P shell, but splits the $1F$ and $1G$ shell into two subshells each [29], as indicated in Fig. 1. The separation of these subshells can therefore be taken as a measure for the strength of the electron-lattice interaction. The cuboctahedral cluster, though exhibiting a DOS very similar to that of the
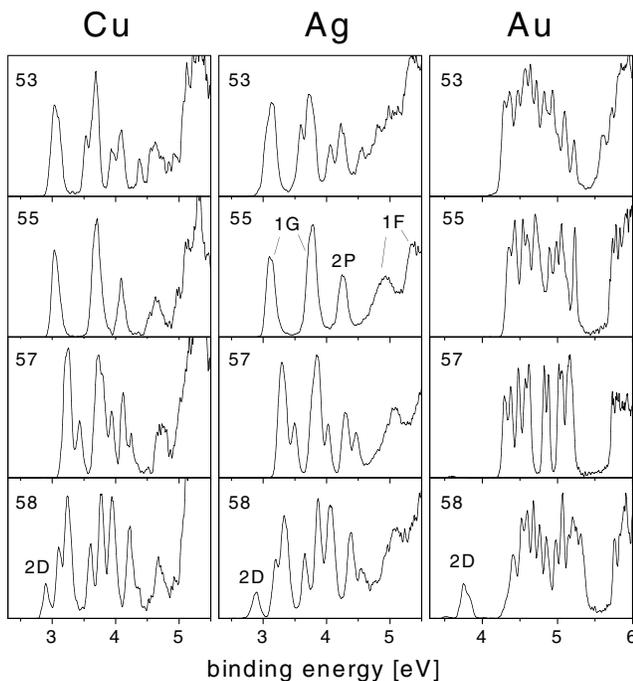

FIG. 1. Photoelectron spectra of Cu_n^-, Ag_n^-, and Au_n^- ($n = 53, 55, 57, 58$) obtained at a photon energy of 6.42 eV.

ICO cluster, can safely be excluded to be present in the experiment because of its significantly higher energy. All other isomers will have a more complex DOS. So, although we cannot exclude that other low-symmetry isomers exist which are energetically closer to the ICO than the ones presented here, the purity of the experimental spectrum demonstrates that the icosahedron is by far the dominant structure for the Cu_{55}^- and Ag_{55}^- clusters produced by our source.

As the atomic symmetry of these two clusters leads to the high degeneracy in their electronic structure [27], it is interesting to see how it will change if the symmetry is perturbed. In Fig. 1 one can observe that if the cluster size is increased or decreased by two atoms, the three upper peaks in the spectra split up. This splitting can be most

(a)

ico   cubo   deca   SC   Morse   glue
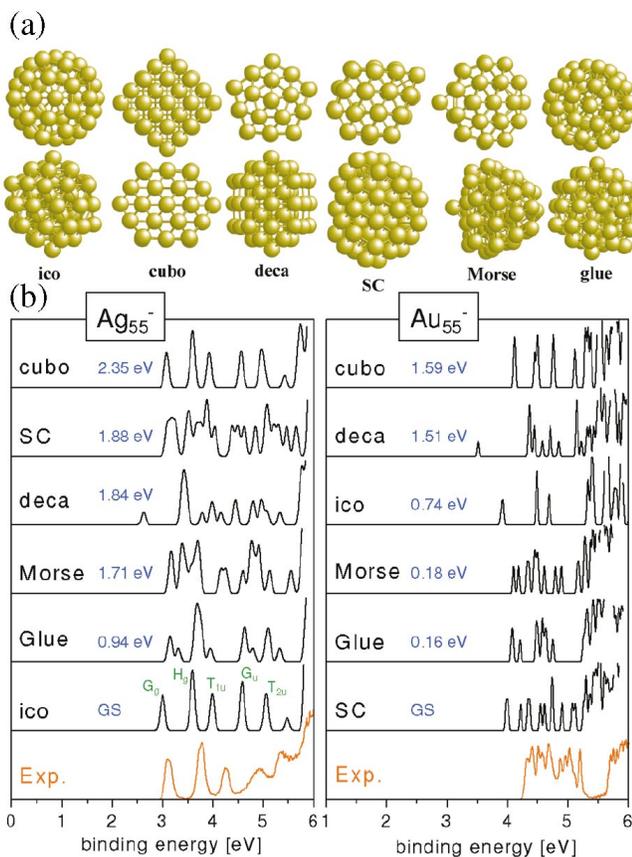
(b)

FIG. 2 (color).   Structures and density of states (DOS) of Ag and Au clusters obtained via density functional calculations. (a) Six candidate structures (displayed are the fully relaxed optimal structures for gold) for Ag_{55}^- and Au_{55}^- representing different structural motifs: closed atomic shell icosahedral (ICO), decahedral (DECA), and cuboctahedral (CUBO) structures, and clusters optimized previously by classical Sutton-Chen (SC), Glue, and short ranged Morse potentials; (b) DOS of the six structures (black curves) compared to the experimental photoelectron spectra (red curves) for Ag (left panel) and Au (right panel). The numbers denote the energy difference to the most stable structure (GS).
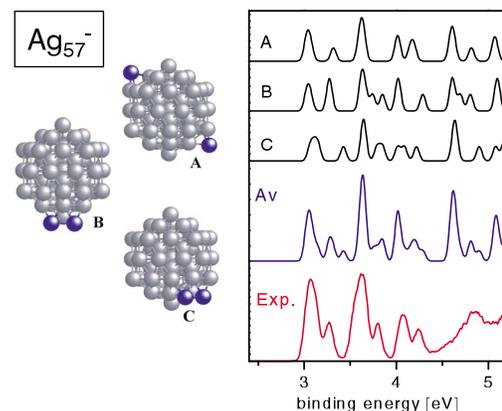
easily understood for the case of the T_{1u} (2P) orbital. Assuming that the geometries of the clusters are based on the 55-atom icosahedron, Ag_{53}^- has two vacancies in the outermost atom shell and therefore a slightly oblate shape, whence Ag_{57}^- has two adatoms and is prolate. In the case of a P-type orbital this will lead to a splitting into the $P_x^2 P_y^2 P_z^2$ subshells, with 1:2 and 2:1 intensity ratios of the lower:higher binding energies for oblate and prolate shapes, respectively. This is exactly what one can observe in Fig. 1. The same can be seen in the theoretical spectra of Ag_{57}^- in Fig. 3, where the calculated DOS of the three lowest energy isomers is shown. Interestingly the splitting of the shells is more pronounced in the calculation than in the experiment. This could be a temperature effect: in the calculation the geometries are fully relaxed at 0 K; here the attached atoms produce some distortion of the icosahedral core and thereby some additional perturbation of the shell structure. In the experiment the finite cluster temperature (about 150–250 K) will probably lead to a larger average bond length of the surface atoms and therefore to a reduced effect on the icosahedral core. Additionally the attached atoms will probably be more mobile than the energy differences between the different isomers indicate. In order to check this we show a simple average of the three calculated spectra as well. The better agreement of this averaged spectrum with the measured one indicates that indeed more than one isomer is present in the experiment, which is probably due to a constant movement of the attached atoms on the icosahedral core.

Let us now turn to the case of gold. The experimental spectrum of the Au_{55}^- cluster is drastically different from those of Ag_{55}^- and Cu_{55}^- (Fig. 1). The visible part of the ``s band'' is highly structured, but does not show any trace of a shell pattern. This can be taken as direct evidence that a

FIG. 3 (color).   Three icosahedral-based candidate structures (A, B, C) of Ag_{57}^- and their calculated DOS as well as an average of A, B, and C (Av) and the experimental photoelectron spectrum (Exp.). The calculated energies of the isomers A and B with respect to the ground-state isomer C are 0.63 and 0.23 eV, respectively.

free Au_{55}^- does not adopt icosahedral or cuboctahedral symmetry. Indeed from the computations we find several low-symmetry structures (SC, GL, MO) for Au_{55}^- below the ICO. The calculated DOS of these isomers are in a qualitative agreement with the measured spectra, exhibiting no significant level bunching. Perfect agreement cannot be expected, as spin-orbit coupling, which is not taken into account in the calculation, will further perturb the DOS. Additionally, one cannot assume that the SC isomer is the true ground-state of Au_{55}^-, given the vast amount of possible low-symmetry structures (in a previous calculation using semiempirical potentials 360 disordered isomers have been identified that were energetically favorable to the ICO [30]). Nevertheless, both our experiment and our calculation give strong evidence for a low-symmetry ground-state of Au_{55}^-. So why are gold clusters so different from silver or copper clusters? The answer is found by comparing the results of a nonrelativistic calculation with those of a scalar-relativistic one. It turns out that a fictitious, nonrelativistic Au_{55}^- behaves very similar to Cu_{55}^- or Ag_{55}^-, having a clear ICO ground-state and an almost identical DOS. Only in the scalar-relativistic calculation the lower symmetry isomers are preferred, which is due to a change in the nature of the interatomic bonding. The Au atom is known to be "the most relativistic element below Fermium" [31], displaying a strong outer shell ($6s$) contraction and a reduced $5d$–$6s$ energy gap. This leads to significant s-d hybridization and direct d-d bonding effects, which for instance are also responsible for the anomalous, planar ground-state structures of anionic Au_n^- clusters up to about $n = 12$ [11–13]. The most obvious consequences of these relativistic effects are a shortening of the interatomic bond lengths and a drastic increase of the bulk modulus. In a calculation of the Au_2 potential energy curve we have obtained an increase of the curvature from 5.3 $eV/Å^2$ to 11.6 $eV/Å^2$ when including relativistic effects. The same trend was reported earlier for the calculated bulk modulus of crystalline Au, where a relativistic treatment increased the value from 108 to 182 GPa [32]. A recent general study of metal cluster structures demonstrated that it is mainly this high bulk modulus which leads to the different behavior of gold and silver clusters [30].

The fact that Au_{55}^- prefers a low-symmetry structure can therefore be clearly identified as a relativistic effect. This demonstrates the important influence of relativity on the structure of mesoscopic heavy atom particles.

*Electronic address: bernd.von.issendorff@uni-freiburg.de

[1] W. de Heer, Rev. Mod. Phys. **65**, 611 (1993).
[2] T. P. Martin, Phys. Rep. **273**, 199 (1996).
[3] M. Haruta, Catal. Today **36**, 153 (1997).
[4] A. Sanchez *et al.*, J. Phys. Chem. A **103**, 9573 (1999).
[5] J. F. Hainfield, Science **236**, 450 (1987).
[6] W. L. Barnes *et al.*, Nature (London) **424**, 824 (2003).
[7] C. Y. Cha *et al.*, J. Chem. Phys. **99**, 6308 (1993).
[8] H. Handschuh *et al.*, J. Chem. Phys. **102**, 6406 (1995).
[9] J. Tiggesbäumker *et al.*, Chem. Phys. Lett. **190**, 42 (1992).
[10] V. Bonacic-Koutecky *et al.*, J. Chem. Phys. **110**, 3876 (1999).
[11] H. Häkkinen *et al.*, Phys. Rev. Lett. **89**, 033401 (2002).
[12] F. Furche *et al.*, J. Chem. Phys. **117**, 6982 (2002).
[13] H. Häkkinen *et al.*, J. Phys. Chem. A **107**, 6168 (2003).
[14] X. Li *et al.*, Science **299**, 864 (2003).
[15] D. Reinhard *et al.*, Phys. Rev. B **55**, 7868 (1997).
[16] L. D. Marks, Rep. Prog. Phys. **57**, 603 (1994).
[17] G. Alameddin *et al.*, Chem. Phys. Lett. **192**, 122 (1992).
[18] K. J. Taylor *et al.*, J. Chem. Phys. **96**, 3319 (1992).
[19] M. Astruc *et al.*, Phys. Rev. B **66**, 041404(R) (2002).
[20] G. Wrigge *et al.*, Phys. Rev. A **65**, 063201 (2002).
[21] S. Krückeberg *et al.*, Eur. Phys. J. D **9**, 169 (1999).
[22] A. Herlert *et al.*, J. Electron Spectrosc. Relat. Phenom. **106**, 179 (2000).
[23] R. N. Barnett and U. Landman, Phys. Rev. B **48**, 2081 (1993).
[24] J. P. Perdew *et al.*, Phys. Rev. Lett. **77**, 3865 (1996).
[25] N. Troullier, and J. L. Martins, Phys. Rev. B **43**, 1993 (1991).
[26] The Cambridge Cluster Database, D. J. Wales *et al.*, see http://brian.ch.cam.ac.uk/CCD.html, and references therein.
[27] We call these structures icosahedral although the partial occupation of the uppermost G_g shell leads to a Jahn-Teller (JT) deformation; due to the rigidity of the lattice this deformation is, however, very small. In our unconstrained MD optimization we find JT-induced changes of the bond lengths of less than 2%; this results in a total width, e.g., of the G_g derived band of only 0.04 eV.
[28] T. H. Upton, Phys. Rev. Lett. **56**, 2168 (1986).
[29] H. P. Cheng *et al.*, Phys. Rev. B **43**, 10647 (1991).
[30] J. M. Soler *et al.*, Phys. Rev. B **61**, 5771 (2000).
[31] P. Pyykkö, Chem. Rev. **88**, 563 (1988).
[32] C. Elsässer *et al.*, J. Phys. Condens. Matter **2**, 4371 (1990).